Enhancement of electromechanical properties of natural rubber by adding barium titanate filler: An electro-mechanical study

Ajeet Kumar[1], Dilshad Ahmad[1], Karali Patra[1] and Mokarram Hossain[2]*
[1]Department of Mechanical Engineering, Indian Institute of Technology Patna, India
[2]Zienkiewicz Centre for Computational Engineering, College of Engineering, Bay Campus, Swansea University Swansea, UK
[1]ajeet.pme15@iitp.ac.in, [1]dilshad.pme14@iitp.ac.in, [1]kpatra@iitp.ac.in,
[2]mokarram.hossain@swansea.ac.uk

Abstract
Natural rubber is one of the most potential electro-active polymers (EAPs) for sensors, actuators, and energy harvesting applications. Enhancing the characteristic properties of polymers by reinforcing with fillers that possess multifunctional attributes have attracted considerable attention. In the present study, barium titanate (BT) reinforced natural rubber (NR) composite is prepared by using two-roll mill mixing. Afterwards, mechanical, electrical, and electromechanical properties of the composites are extensively analyzed by reinforcing different amounts of barium titanate into the matrix of natural rubber. The fabricated dielectric composite shows excellent properties such as high dielectric constant, low dielectric losses, high dielectric breakdown strength, and extreme stretchability. It is observed that as the filler loading reaches the value of 11 parts per hundred rubber (phr), maximum agglomeration of the particles occurs. Maximum stretchability and highest ratio of dielectric constant to elastic modulus are obtained at 8 phr of barium titanate fillers and at the loading, a maximum actuation strain of 11.24% is achieved. This study provides a simple, economical and effective method for preparing enhanced mechanical, electrical and electromechanical properties of natural rubber composites, facilitating the wide applications of dielectric materials as actuators and generators.

Keywords: Natural rubber; Barium titanate; Dielectric constant; Elastic modulus; Actuator; Generators.

1. Introduction

Dielectric elastomers are a class of materials that can be used as smart materials with a wide application area ranging from soft robotics, artificial muscles sensors, actuators, and energy harvesting devices [1–4]. Dielectric elastomers can transfer electrical energy into mechanical energy (actuator mode) and vice versa (generator mode). In actuator mode, large deformation of the dielectric elastomer can be obtained by applying electric fields on the compliant conductive electrodes coated on the opposite surfaces of a thin film [5–9]. In generator mode, when a stretched and charged coated dielectric elastomer is relaxed, similar charges are attracted together and opposite charges are pushed apart that generally increase voltage or electrical energy [10,11]. Such exotic phenomena of dielectric elastomers attracted many researchers to look for potential polymers that can be utilized in various applications.

In the present scenario, research works are being carried out mainly on commercially available elastomers such as acrylic-based elastomers [12–16], silicone-based elastomers [17,18], and natural rubber [6,19,20]. VHB, an acrylic based elastomer, is one of the most widely explored dielectric elastomer materials within the scientific community. It has many advantages such as large stretchability, low elastic modulus, good electromechanical properties [3,21,22]. Instead of these favourable properties, it has several limitations i.e., high viscoelasticity, high loss of tension, high

*corresponding author
Email ID – kpatra@iitp.ac.in

operating voltage. Also, its adhesive nature [23] hinders practical applications in different areas such as biomedical, low voltage sensors, etc. [24]. Another important disadvantage of VHB is that the dielectric constant of the polymer decreases significantly with the increase in stretch ratios [25]. Silicone elastomers, on the other hand, are also being used in dielectric elastomer applications [26–30]. They are available commercially or are fabricated by mixing part A and part B liquid mixture. Part A is the silicone liquid and part B is the curative agent by which it can be cast into the desired thickness. Silicones have relatively less viscosities, low sensitivities to temperature with high stretchability [31]. However, they have very low value of dielectric permittivity.

Natural rubber (NR) is one of the most promising electro-active materials thanks to its inherent properties such as high energy density, low viscoelastic losses, high elasticity, less temperature sensitivity, high tearing resistance, low heat build-up, and high fatigue resistance [32-35]. These properties are most desirable for the dielectric elastomer-based applications such as in actuators and generators [35]. Several existing works have already proved that natural rubber is one of the best alternatives among different dielectric elastomers for generator mode [36,37]. In comparison to the research on commercially available acrylic and silicone-based elastomers, less attention has been paid to synthesizing novel polymers for generator mode. In contrast to acrylic and silicone-based polymers, natural rubbers have excellent mechanical and electrical properties such as low sensitivity to moisture, and high durability over time [17]. However, it has a low dielectric constant with moderate dielectric losses [36], low dielectric breakdown strength and comparatively higher elastic modulus [32]. Due to these unfavourable properties, applications of natural rubber and other dielectric elastomers as electromechanical transducers are still challenging.

Recently, several research works have been attempted to synthesis dielectric elastomers composites filled with high dielectric constant fillers [38–43] to improve dielectric and electromechanical properties. Kumar et al. [29] fabricated BT filler silicone composite cured in the presence of electric field to improve the overall electromechanical property of composite. Yang et al. [38] fabricated natural rubber composites with surface modified TiO_2 as a filler and observed moderate increase in the dielectric constant of 3.48 at 50 phr of TiO_2 with maximum actuation strain of 12.30% at 10 phr of TiO_2. Yin et al. [44] fabricated polyurethane composites taking barium titanate (BT) as a filler. They experimentally observed that there was an increase in the dielectric constant from 7.4 to 13.6 with a filler content of 50% BT by weight at 1kHz.

In a similar line, attempts have also been made to develop filled natural rubber composite for improving its properties. Ruan et al. [45] improved the electromechanical properties of butyl rubber composite by adding BT filler. They found that there was an increase in dielectric constant from 2.8 to 3.7 with a filler content of 30 wt.% of BT at 1 kHz and actuation strain increases from 0.5% to 3.5% with a filler content of 30% of BT by weight at 20 kV. The results showed that there was not much improvement in the dielectric constant and actuation strain for the rubber composite. Yung et al. [46] fabricated natural rubber composites by adding barium titanate and dioctyl phthalate plasticizer

(DOP) and observed enhancement of the dielectric constant. However, the dielectric breakdown strength decreases from 60.5 MV/m to 22.0 MV/m by adding 30 phr of DOP and 50 phr of BT. Moreover, they didn't demonstrate the stress relaxation behaviour of the composite which is a very important aspect as the dielectric elastomers goes under large deformation in actuators and generators modes of applications. González et al. [47] prepared natural rubber composites by using a hydroxylated barium titanate filler (BaTiO3-OH). They achieved high elongations between 874% to 935% before the failure of the composite. However, dielectric constant of the natural rubber composite is reduced compared to the pure natural rubber. Also, the obtained dielectric breakdown strength of the composite was less as compared to the pure natural rubber.

Jose et al. and Salaeh et al. [48,49] fabricated carbon nanotube (CNT) filled natural rubber composite and found that CNT reinforcement enhanced the mechanical properties of natural rubber. Jose et al. reported a 55% increase in tensile strength and 1.6 units increase in the dielectric constant after the reinforcement. The addition of CNT increases the dielectric constant of the composite but the dielectric breakdown decreases [50,51]. Yang et al. [38] added titanium-oxide (TiO_2) in natural rubber and conducted electrical and mechanical characterizations of the fabricated composites. They reported increases in dielectric constant from 3.14 to 3.56 with the change in BT filler content of 50 phr. Tian et al. [52] used graphene oxide (GO) as a high constant filler to fabricate natural rubber composite by using latex. The dielectric constant of natural rubber latex was quite high, however, it results in a poor elasticity [53]. Ideally, dielectric elastomers should have a low elastic modulus, low dielectric loss, and high dielectric constant as the actuation strain is directly proportional to the dielectric constant and elastic modulus [54].

Despite many researchers have investigated the mechanical and electrical characterizations of NR composites, to the best of author's knowledge, a complete mechanical, electrical, and electromechanical characterization at different reinforcement of fillers is still a field to be investigated in details. Therefore, in the current investigation, barium titanate reinforced natural rubber composites are synthesized and comprehensive mechanical, electrical and electromechanical characterizations are conducted. To this end, standard mechanical experiments like stress-strain, loading-unloading, stress relaxation tests are conducted. Moreover, variation of the dielectric constant with temperature and frequency are analyzed. All the aforementioned test established a strong dependency of filler content on natural rubber. Also, the aim of this contribution is to achieve maximum actuation strain for natural rubber reinforced composites. Hence, different phr of filler particle (BT) is added and actuation tests are conducted systematically.

The current work is organized as follows: In Section 2, a detailed discussion about material, its synthesis and characterization methods are explained. In Section 3, experimental outcomes for mechanical and electrical tests are elaborated. In the same section, morphological study of fractured surface through SEM is analyzed and discussed. A final Section 5 presents a brief summary of the current work.

2. Experimental

2.1 Preparations of natural rubber/BT composites

Indian standard Natural rubber (ISNR) of Indian standard grade ISNR 3 CV was used in the current study. Barium titanate nanopowder having a grain size less than 100 nm (supplied by Sigma Aldrich) was used to reinforce the polymer matrix. Stearic acid and zinc oxide (ZnO) (supplied by Sigma Aldrich.) were used as activators. Cyclohexyl benzothiazyl sulphenamide (CBS) and tetra methyl thiuram disulphide (TMTD) were used as an accelerator. N-(1,3-dimethylbutyl)-N'- Phenyl-P-phenylenediamine (6PPD) and Sulphur were used as an anti-degradant and vulcanizing agent, respectively. Before compounding, barium titanate powder was dried in a vacuum oven at 100℃ for 24 hours. Figure 1 shows the scanning electron microscope (SEM) image of powder BT filler particles. Natural rubber/barium titanate (NR/BT) composites compounding was carried out on a two-roll mill at room temperature. All the reagents which were added in a sequence are shown in the compounding formulation Table 1. Rubber block was cut into small pieces and was masticated for 5 minutes first, followed by additional ZnO and stearic acid milled for 2 minutes. Accelerators, CBS, and TMTD were subsequently added into the mixture and milled for another 1 minute. Further, antioxidant 6 PPD was added into the mixture and milled for 1 minute. Finally, vulcanizing agent, Sulphur followed by filler particles BT were added and milled for 2 minutes each. Further, vulcanization was carried out at temperature of 150℃ in the compression molding machine. The temperature value of 150℃ is selected as it is the optimum curing temperature (T_{90}) of Sulphur. For obtaining desirable thickness of NR/BT composites, say 1 mm for tensile test specimen and dielectric properties test specimen, a mold was used having 1 mm thickness which was kept between the two plates of the compression molding machine. However, for making specimens for electromechanical experiments, the blend was kept directly between the two plates of compression molding machine so as to obtain the desirable thickness of 100 μm. The arrangement of filler particles in the interfacial space between the two polymer chains and vulcanization of natural rubber with Sulphur is shown in Figure 2.

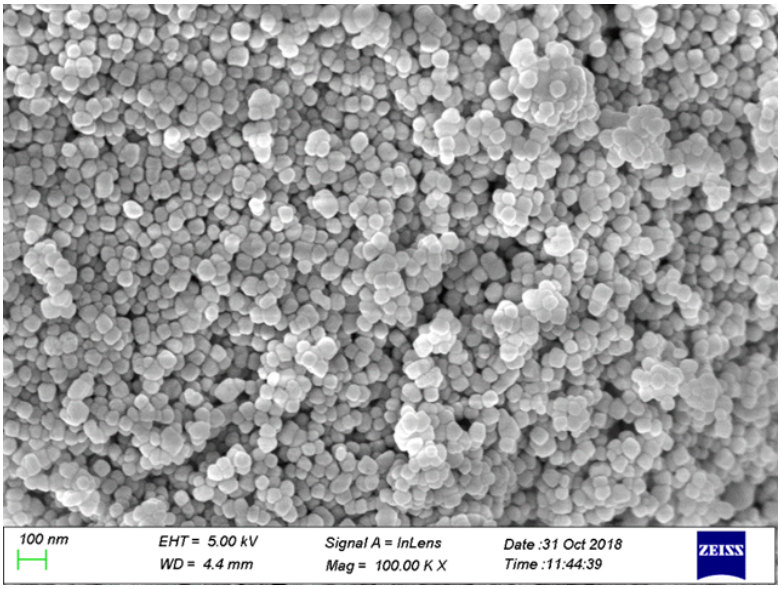

Figure 1: SEM image of BT powder

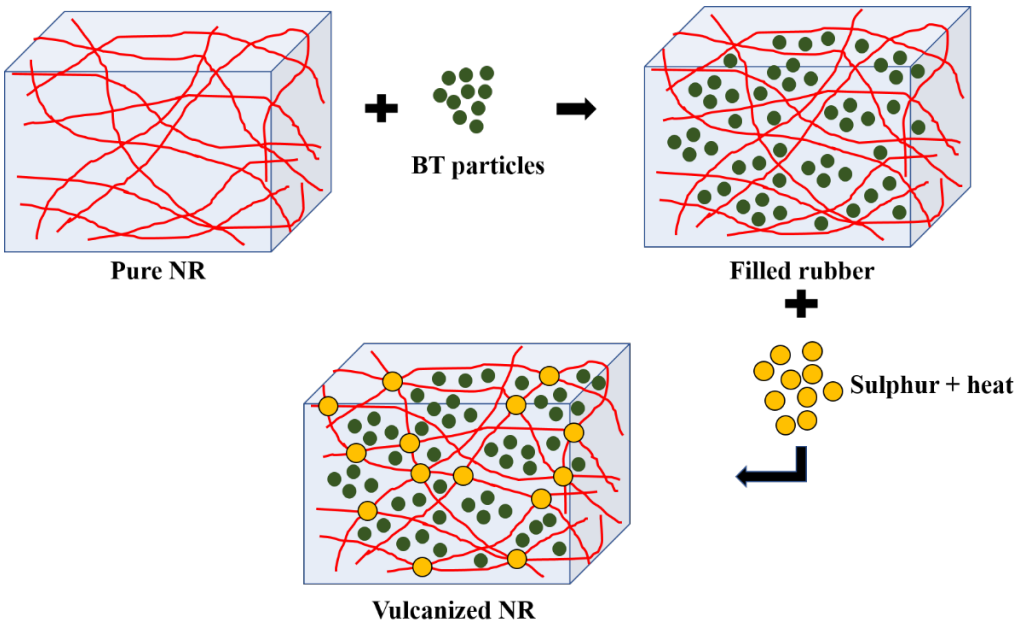

Figure 2: Schematic arrangement of barium titanate and sulphur particles in the polymer matrix

2.2 Measurement Technique

Tensile tests were carried out with double dumbbell-shaped specimens as per ASTM D412 standard as shown in Figure 3(a). A universal testing machine (Zwick/Roell Z010) with a maximum load capacity of 2.5 kN is used to test the specimen as shown in Figure 3(b). The cross-head speed of 50 mm/min having a strain rate of 0.025 per second at room temperature of 25±3℃ is used for the tests. Dielectric elastomer actuators and generators are generally operated in this range of strain rate [55, 56]. Data were obtained and analyzed by using TestXpert II build-in software of Zwick/Roell Z010. All the tests were conducted at least three times to ensure good reproducibility. The vertical error bars

in experimental results show the standard deviations of these measurements. Further, scanning electron microscopy (SEM) images of fractured surfaces were taken by using scanning electron microscopy technique (Gemini SEM 500, Germany) to study the morphology of the fabricated composites. To investigate the viscoelastic nature of NR/BT composites, cyclic loading-unloading tests were conducted on a universal testing machine (Zwick/Roell Z010). We conducted cyclic loading-unloading tests by straining the samples up to a maximum strain of 200%. This deformation limit is well enough for dielectric elastomers as they are being used in soft robotics and energy harvesting mechanisms. To investigate the equilibrium states, stress relaxation tests were carried out at a holding strain of 200% and a relaxation time of 600 seconds was selected.

For the measurements of dielectric properties of the fabricated composite, Novocontrol spectroscopy (Alpha-A) was used at a one-volt (1V) signal within frequency range of 1 Hz to 1 MHz at room temperature as shown in Figure 4. The NR/BT composite was cut into a circular shape having a diameter equal to the gold coated electrode diameter (20 mm) of the Novocontrol spectroscopy analyzer and fixed into the active sample cell of the setup as shown in Figure 4 (a). An in-built software, WinDETA was used to obtain data from Novocontrol spectroscopy. Results related to dielectric properties obtained from the tests were analyzed in the software. All the tests were conducted at least three times to ensure good reproducibility.

Further, actuation tests were carried out using high voltage DC source. The schematic diagram of the setup is shown in Figure 5. The electric test set up comprises of high voltage DC source (Ionics Power Solution Private Limited), high resolution camera (Logitech), and a sample holder, shown in Figure 5. To measure the actuation strain, the natural rubber composites were fixed in a circular holder. Samples having a thickness of 100 μm were fixed in a circular frame of 50 mm internal diameter. Carbon conductive grease (MG chemicals) was used as a compliant electrode. A circular shaped, 10 mm diameter of conductive grease were coated on both sides of the film. The prepared circular actuator specimen was connected to the two terminals of high voltage DC supply. The circular actuator was continuously ramped at a constant voltage ramp rate of 100−200 V/s. The actuation of the circular actuator was recorded by using a high-resolution camera. Further, the recorded videos were converted into images with the frame rate of 2 frames per second. High resolution images were then analyzed by using 'ImageJ' software.

The planar actuation strains were calculated by using the relation, $S_p = (A_2 - A_1)/A_1 \times 100$, where S_p is the planar actuation strain, A_2 is the actuated area and A_1 is the initial coated electrode area. The calculated area strains reported in the present work are the average of at least three repetitions of the specimen for a particular condition. Further, electromechanical sensitivity (β) is also calculated for the NR/BT composites which is the ratio of dielectric constant to the elastic modulus of the respective composites.

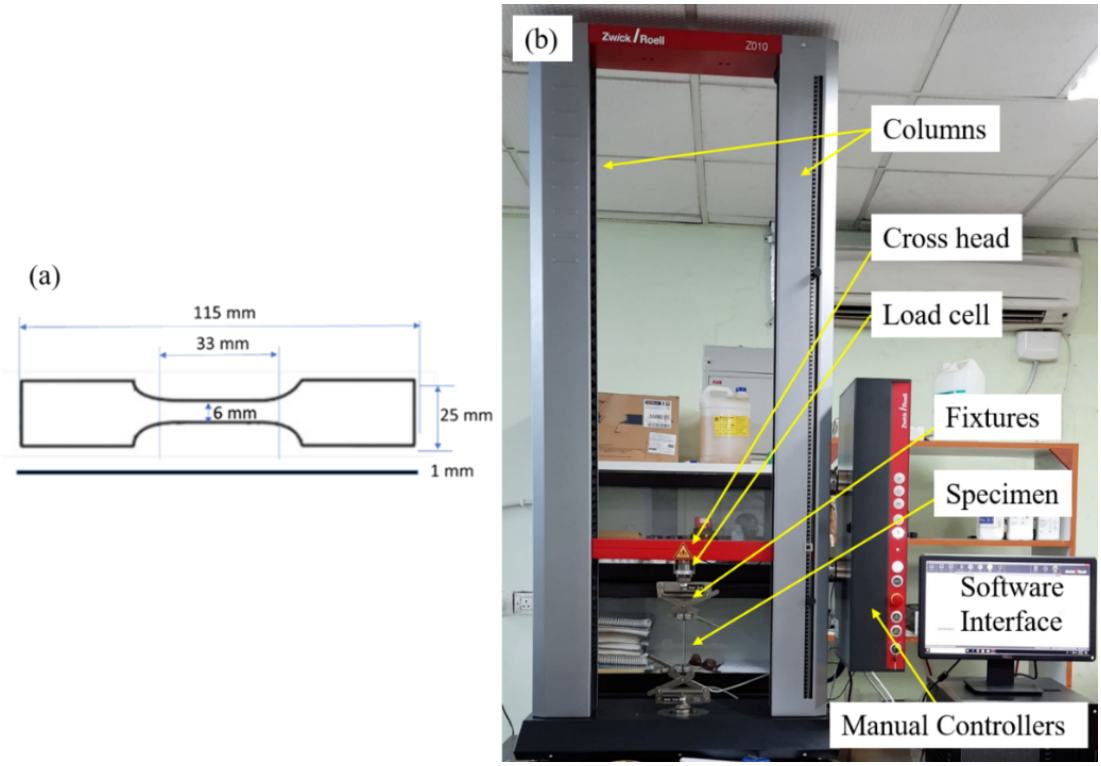

Figure 3: (a) Tensile test sample dimensions, (b) Universal testing machine setup with specimen

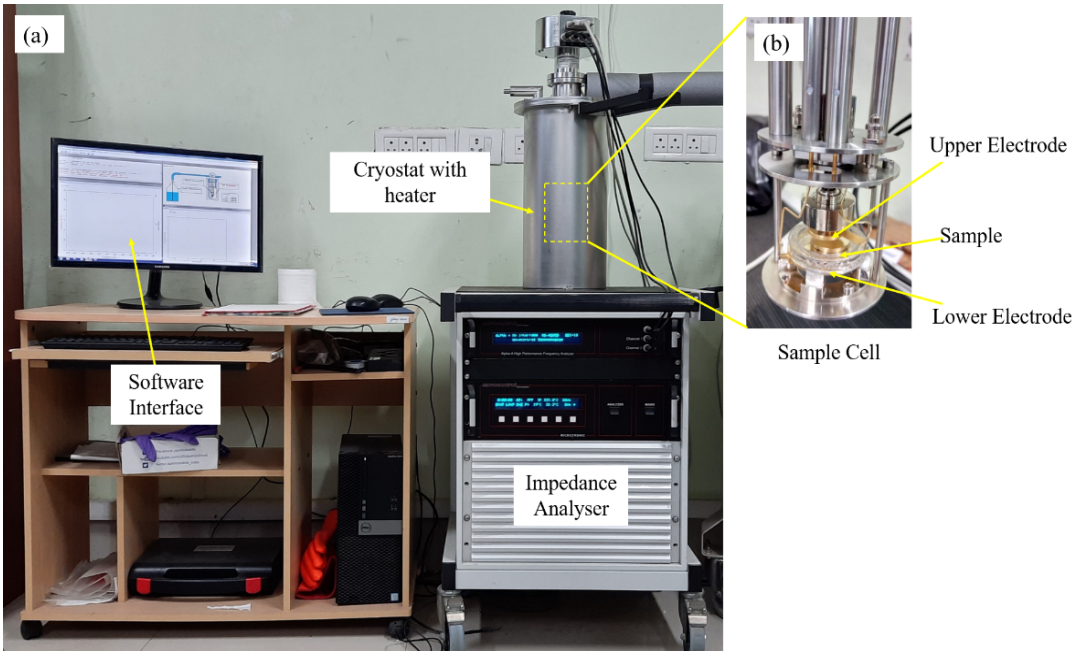

Figure 4: (a) Spectroscopy setup used for dielectric properties measurements, (b) Active sample cell with upper and lower electrodes

Table 1: Compounding formulation for fabrication of NR/BT composite (in phr[a])

Reagents	NR/$BaTiO_3$ (0 phr)	NR/$BaTiO_3$ (2 phr)	NR/$BaTiO_3$ (5 phr)	NR/$BaTiO_3$ (8 phr)	NR/$BaTiO_3$ (11 phr)
NR	100	100	100	100	100
Stearic acid	2.0	2.0	2.0	2.0	2.0
ZnO	5.0	5.0	5.0	5.0	5.0
CBS	1.0	1.0	1.0	1.0	1.0
TMTD	1.0	1.0	1.0	1.0	1.0
6 PPD	1.0	1.0	1.0	1.0	1.0
Sulphur	1.0	1.0	1.0	1.0	1.0
$BaTiO_3$	0	2.0	5.0	8.0	11.0

[a]phr = parts per hundred rubber, by weight

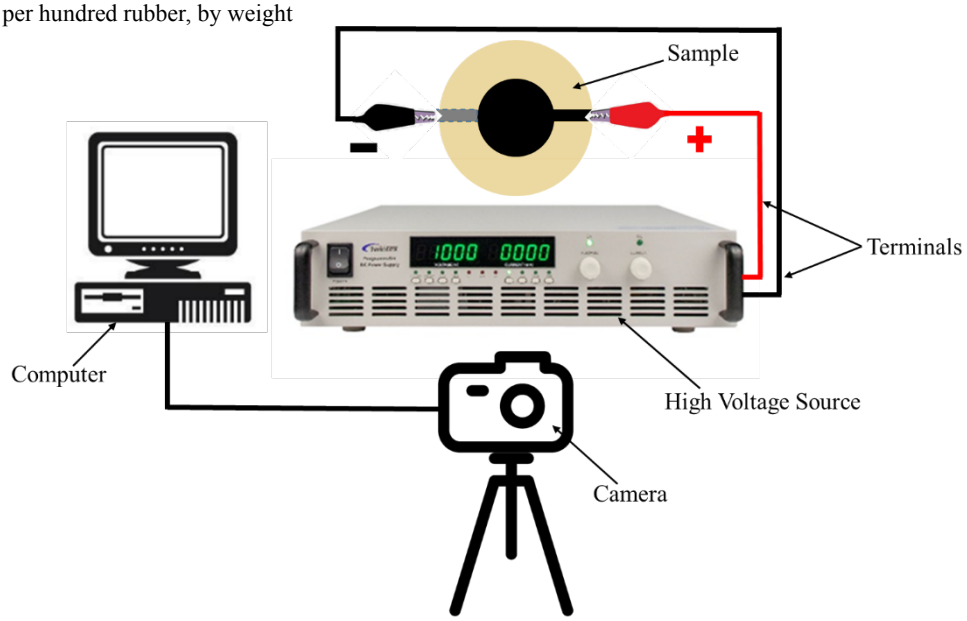

Figure 5: Actuation strain measurement setup for planner actuation strain measurement of NR/BT composite

3. Results and discussions

3.1 Mechanical properties of natural rubber composites

Stress-strain curves of unfilled natural rubber and natural rubber composites are plotted in Figure 6(a). It can be easily seen that as the filler content of BT increases, tensile strength also increases. Higher tensile strength attributes to the fact that as the filler content fills the space between polymer chains, it

restricts the chains to slip on each other. The highest tensile strength of the prepared NR/BT composite is 15.5 MPa at 11 phr. It is followed by 14.6 MPa at 8 phr. These values are 60% and 52% more than that of the tensile strength value of pure NR, respectively. Initially, the fillers are well dispersed up to 8 phr of BT in NR but as reinforcement increase from 8 to 11phr, crosslink density increases, and agglomeration of particles takes place. Stretchability also increases with the increasing amount of BT and is the maximum when filler loading is 8 phr. Further increase in the filler content decreases the stretchability because of agglomeration of fillers, i.e., optimum limit of crosslink density, see Yang et al. [38].

Table 2: Elastic modulus and failure stretch % of NR/BT composites and comparison with previous works

Natural rubber	Filler	Filler content	Elastic modulus (MPa)	Failure stretch (%)
Smoked sheet (RSS No. 1) [38]	TiO_2	0 phr	1.10±0.06	477
		10 phr	0.99±0.08	445
		30 phr	1.23±0.09	475
		50 phr	1.56±0.12	471
Liquid NR latex [47]	BT-OH	0 phr	–	815
		0.25 phr	–	825
		0.50 phr	–	840
		1.00 phr	–	810
		5 phr	–	805
Smoked sheet [46]	BT	0 phr	0.24±0.021	1750
		10 phr	0.27±0.034	1250
		50 phr	0.41±0.023	750
This work	BT	0 phr	0.71±0.03	785±22
		2 phr	0.72±0.02	810±25
		5 phr	0.75±0.05	815±20
		8 phr	0.68±0.04	835±22
		11 phr	0.74±0.03	815±18

The variations of elastic modulus of the NR/BT composite with filler content are shown in Figure 6 (b). It is observed that the elastic modulus increases with increase in filler content from 2 phr to 5 phr.

Further increase in filler content upto 8 phr, BT particles hinder the polymer chain to form crosslink with Sulphur particles during the vulcanization process. Hence, crosslink density decreases. As crosslink density is directly proportional to elastic modulus [57], elastic modulus also decreases at 8 phr BT. On further increase, an agglomeration of fillers results into increase in the elastic modulus of the NR/BT composite [58]. Also an increase in filler content more than the threshold value results in agglomeration of filler which doesn't affect the crosslink density. Hence, again elastic modulus increases [59] which is much similar to other research groups. Their works are well illustrated in Table 2 [38,46,47].

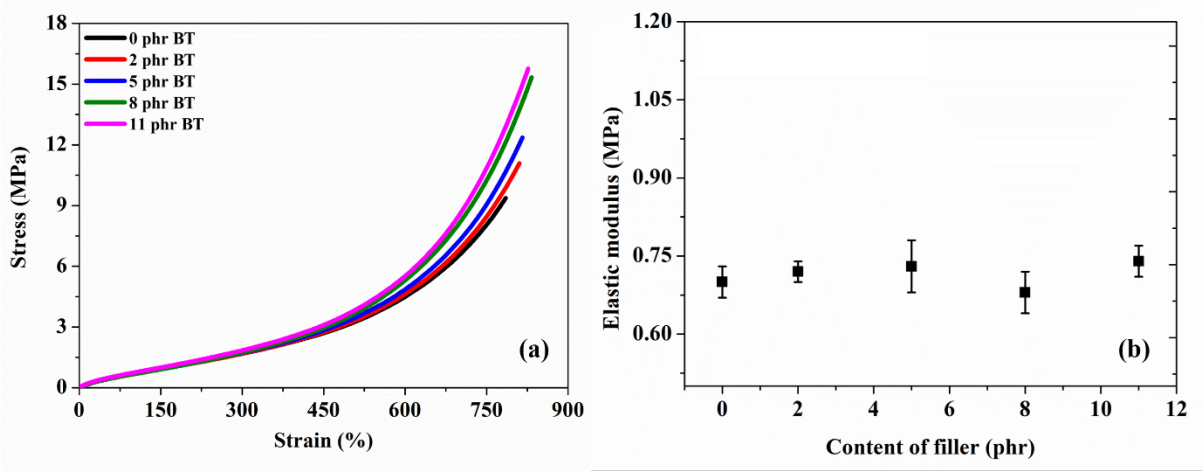

Figure 6: (a) Stress strain curves of NR and NR/BT composite, (b) elastic modulus of the NR/BT composite at different filler content

3.2 Loading-unloading cyclic tests.

In several applications of dielectric elastomers such as in actuators and generators, materials undergo many loading-unloading cycles exhibiting hysteresis losses. Therefore, to investigate hysteresis of synthesized composites, cyclic loading-unloading tests were carried out on a universal testing machine with a fixed strain rate of 0.025 per second. Such a low strain rate was chosen because most of the applications work under a low strain rate [2,60,61]. We performed single loading-unloading curves for each NR/BT sample with a repetition of three to measure hysteresis loss with change in filler loading. The area enclosed under the loading-unloading curve represents the hysteresis loss during the cycle. From Figure 7, it is observed that the dissipative loss slightly increases with increasing filler loading. This is because pristine natural rubber chains are free to slide on other chains, which are constrained by the presence of BT particles in between the rubber chains. This results in the increase of dissipative energy as the friction between filler particles and polymer chains increases with increasing filler loading as shown in Table 3. Kaltseis et al. [37] observed hysteresis loss of 2.3% and 7.0% for Oppoband 8003 and ZruElast A1040, respectively. They used commercial grades natural rubber such as Oppo band 8003 and ZruElast A1040.

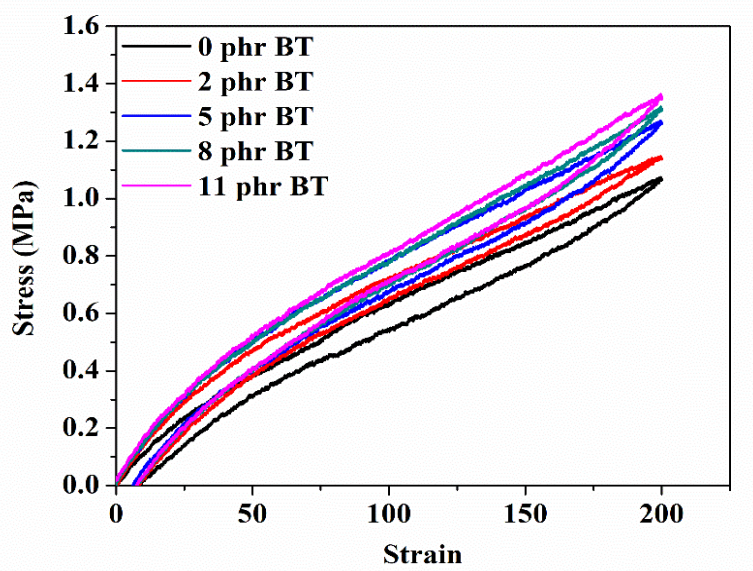

Figure 7: Hysteresis cycles of NR/BT composite with different amount of BT

Table 3: Energy loss due to loading and unloading of NR/BT composites

NR Sample (phr)	Stress (MPa) at 200% strain	Loss (%)
0	1.064±0.025	12.72±2.34
2	1.137±0.031	12.79±3.22
5	1.261±0.028	13.15±4.19
8	1.350±0.026	13.41±2.91
11	1.410±0.022	13.39±3.26

3.3 Stress relaxation tests

Stress relaxation is an important phenomenon to understand the viscoelastic property of polymers. To understand the viscoelastic nature and equilibrium stress response of NR/BT composites, stress relaxation tests have been conducted up to 200% strain and then the sample is kept hold at that strain for 10 minutes to attain an equilibrium stress state. Figure 8 illustrates the stress relaxation curves of NR/BT composites for different filler loads. It is observed that the stress for unfilled natural is quickly relaxed compared to filled NR/BT composites. That means, for a particular strain, an unfilled polymer chain will easily attain an equilibrium state of stress in contrast to NR/BT composites. From Table 4 we observed that, as the filler content increases from 0 to 11%, the stress relaxation time also increases. This is since BT particles hinder the movement of free chains responsible for viscous overstress resulting in the increase of the relaxation time for filled polymers. However, at the relaxed state the level of equilibrium stress increases as the filler content increases from 0% to 11%, see also in Table 4.

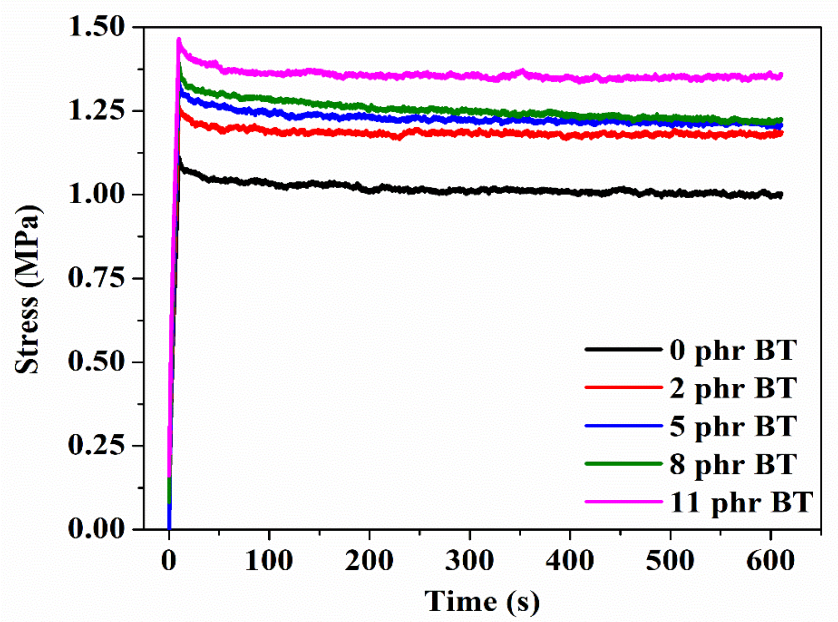

Figure 8: stress relaxation curves of NR/BT composites

Table 4: Stress in the beginning and after 600 seconds of holding time for NR/BT composites with increasing filler loading

NR Sample (phr)	Stress (MPa) at t = 0 second	Stress (MPa) at t = 600 second	Stress Relaxation %
0	1.095±0.032	1.005±0.047	8.22±0.55
2	1.245±0.051	1.185±0.034	4.82±0.21
5	1.310±0.043	1.210±0.029	7.63±0.15
8	1.350±0.035	1.250±0.021	7.40±0.19
11	1.425±0.023	1.365±0.026	4.21±0.25

4. Scanning electron microscopy (SEM) images of fractured surface

Addition of the filler to natural rubbers influences their mechanical properties as discussed in section 3.2. Moreover, it is important to determine the optimum amount of BT particles filled to the NR matrix. So, with the help of scanning electron microscopy, reinforcement of fillers in the polymer matrix can be easily observed. Figure 9 illustrates the SEM images of the fractured surface i.e. the cross-section of natural rubber composites. BT particles are well dispersed in the available space between two NR chains as shown in Figure 9. It can be seen that at a low filler content, the agglomeration of BT particles in the matrix is negligible but as the filler content increases the size and concentration of agglomeration increases and become highest at 11 phr of BT. The yellow circles show the agglomeration of BT particles between the NR polymer chains. The magnified image (400 magnification) of agglomeration of BT particles can be seen in 11 phr of filler.

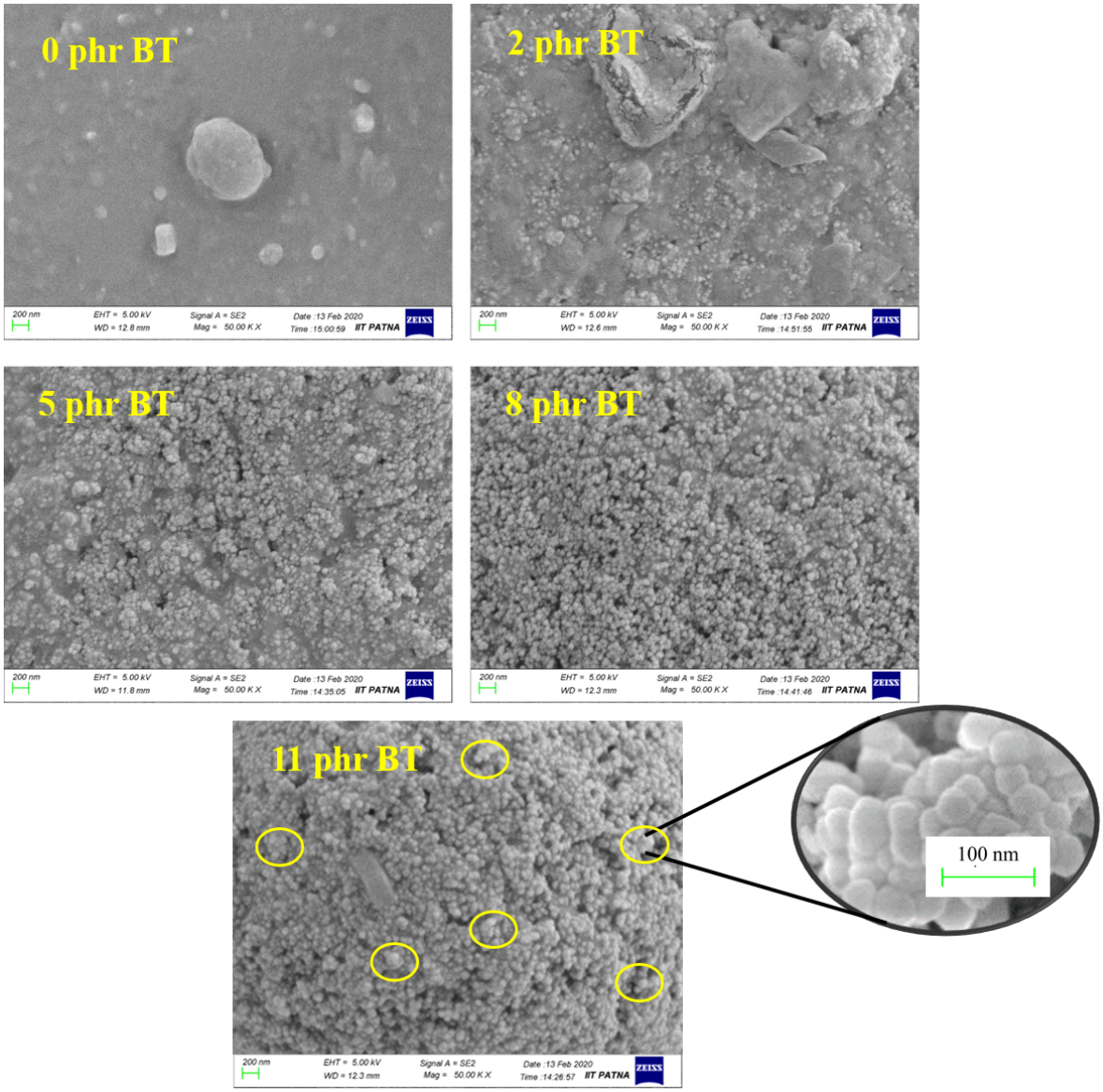

Figure 9: SEM images of fractured surface of NR/BT composites with different phr of BT

5. *Dielectric properties of NR/BT composites*

Barium Titanate (BT) is a type of filler material having very high dielectric constant of 150 at 1 MHz (reported by the supplier, Sigma Aldrich). This high dielectric constant filler is being filled in polymer matrix to enhance their dielectric properties. Figure 10(a) shows the dielectric constant of pure NR and NR/BT composites in frequency range of 10^{-2} Hz to 1MHz with different filler contents of BT particles. As the filler content increases from 0% to 11%, dielectric constant also increases from 2.6 to 3.9 at 1 Hz due to interfacial polymerization, respectively. Figure 10(b) shows the dielectric losses of pure natural rubber and NR/BT composites in a frequency range of 10^{-2} Hz to 1MHz with different filler contents of BT. It is observed that dielectric loss decreases with increasing filler content at low frequency. However, the loss remains constant with the increase of frequency after 10 Hz and it does not vary with a change in the filler content.

With increasing frequency from 10^{-2} Hz to 1 MHz, the dielectric constant decreases as the dipoles are unable to polarize with increasing frequency. However, dielectric loss decreases with increasing frequency which is due to the strong interfacial filler and polymer matrix, which constraints the NR polymer chains, decreases the chain mobility as a result dipole polarization decreases [27]. Figure 11 illustrates the change in the dielectric constant with a change in filler content of NR/BT composites at 100 Hz. On the other hand, dielectric losses decrease with an increase in the filler content. Mechanism of dielectric polarisation dipole lags behind the applied electric field, hence dielectric loss decrease with increasing filler contents as the higher filler NR/BT composites will have more dipoles to polarise. From Table 5, we observed that as the filler content increases, dielectric constant values of the NR/BT composite increase as shown by these works. Yung et al. [46] observed an increase in dielectric constant of NR/BT composites from 3.2 to 3.6 with filler content from 0 phr to 50 phr, respectively at 100 Hz. With respect to these work we observed better dielectric constant of NR/BT composite with 4.2 at 1 Hz.

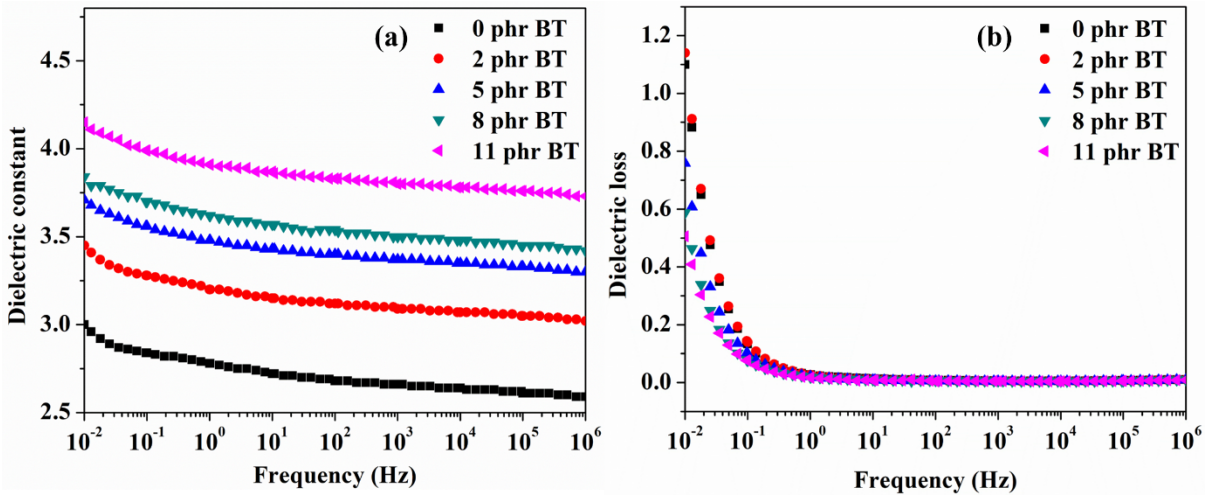

Figure 10: Dielectric properties of NR/BT composites: (a) dielectric constant, (b) dielectric loss

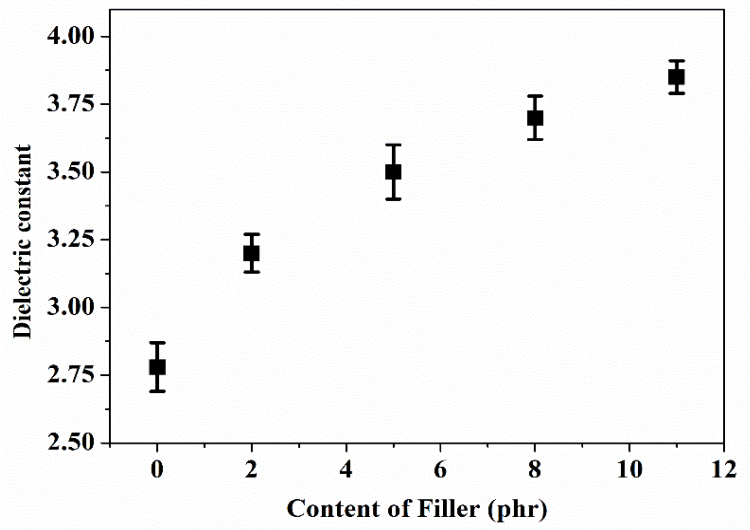

Figure 11: Dielectric constant of NR/BT composite with changing filler content at 100 Hz.

6. Actuation strain and dielectric breakdown strength of NR/BT composites

To investigate the electro-mechanical performances of NR/BT composites, actuation experiments were carried out. A circular actuator was prepared and tests were carried out with different applied electric fields till the dielectric breakdown occurs. As the electric field increases the active area also increases resulting in planar actuations. Figure 12(a) shows the actuation strain of different filler content in NR/BT composites. Actuation strain increases with increasing filler content as it is directly proportional to the dielectric constant of composite and inversely proportional to the elastic modulus as given in equation 1. It shows the electromechanical behaviour of NR/BT composite is directly proportional to dielectric constant of the composites and square of the applied electric filed which is well explained by Krakovsky´et al. [62].

$$S_P = \frac{\varepsilon_0 \varepsilon_r E^2}{Y} \tag{1}$$

where, S_P is the actuation strain, ε_0 is the vacuum permittivity, ε_r is the relative permittivity of a dielectric elastomer, E is the electric field applied and Y is the elastic modulus.

Actuation strain is found to be maximum in the case of 8 phr BT in NR/BT composites. But with a further increase in filler content, actuation strain decreases as the elastic modulus increase simultaneously.

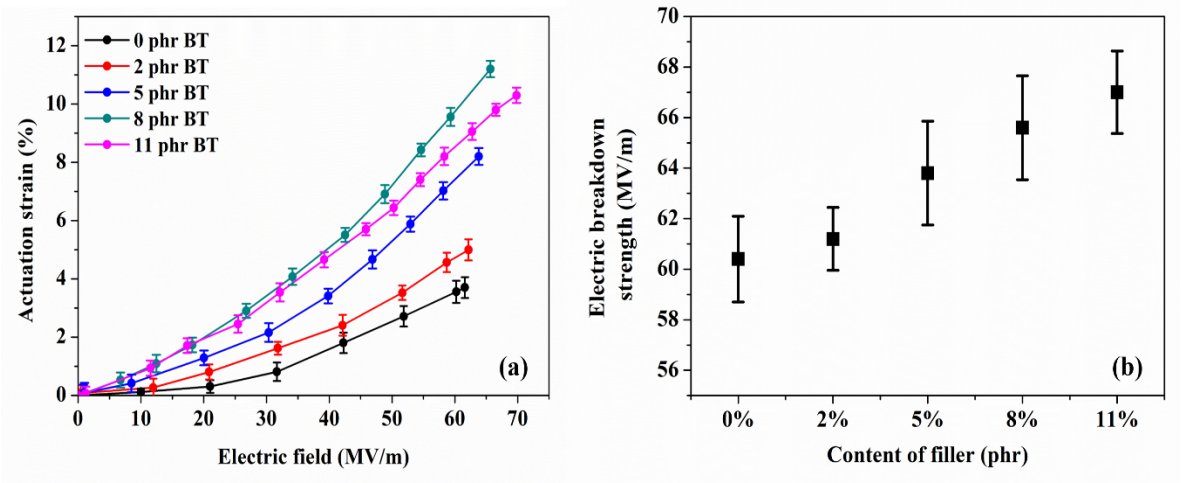

Figure 12: (a) Actuation strain, (b) electric breakdown strength of fabricated NR/BT composites with different filler content of BT

Dielectric breakdown estimates the limit of the electric voltage that an elastomer can sustain before becoming conductive or it fails to bear any electric load. A dielectric elastomer should have a high dielectric breakdown strength so that it can be used in a wide range of electric field. The variation of dielectric breakdown strength with different content of fillers is shown in Figure 12(b). The addition of fillers increases the dielectric breakdown strength of NR/BT composites. Increasing filler content network in polymer chain matrix decreased mobility of NR chains because they are being constrained

by tightly bonded filler nanoparticles and hence, charged are not being carried away which results in enhancement of the dielectric breakdown strength that is also reported by Yung et al. [46].

Table 5 shows the comparison between dielectric constant, electric breakdown strength, planner actuation strain and electromechanical sensitivity (β). Yung et al. used a smoked NR sheet filled with BT particles up to 50 phr. They observed the increase in the dielectric constant up to 3.6 with 50 phr filler loading at 100 Hz while we observed dielectric constant of 3.98 with 10 phr filler loading. We also observed improvement in the actuation strain maximum to 191.95% with 8 phr BT as compared to the pure natural rubber.

Figure 13 shows the plot between the ratio of dielectric constant and elastic modulus denoted by β with changing filler content. The ratio increases with the increase in the filler content resulting in the enhancement of the electromechanical sensitivity (β) up to 8 phr BT. Moreover, actuation strain also increases attending maximum to 11.24%. Beyond 8 phr, the elastic modulus increase is more pronounced in contrast to the increase in the dielectric constant, hence β decreases.

Table 5 : Summary and comparison of some important parameters available in the literature of NR composites

Natural rubber	Filler	Filler content	Dielectric constant (100 Hz)	Electric breakdown strength (MV/m)	Actuated strain (planar area %)	Actuation improved %	β (MPa^{-1})
Smoked sheet (RSS No. 1)[38]	TiO_2	0 phr	2.55±0.08	65±4.8	6.02±0.22	–	2.32
		10 phr	2.73±0.09	67±3.9	9.37±0.25	–	2.75
		30 phr	3.02±0.07	70±4.7	8.30±0.17	–	2.45
		50 phr	3.23±0.08	85±5.8	7.55±0.19	–	2.07
Smoked sheet [46]	BT	0 phr	3.2	60.5±3.5	12.11±1.5	–	13.08
		10 phr	3.3	65.3±3.1	13.94±1.1	–	12.07
		50 phr	3.6	80.1±4.8	12.30±2.1	–	8.68
Liquid	BT-OH	0 phr	3.05	13.00	–	–	–

NR latex [47]		0.25 phr	3.00	16.50	–	–	–
		0.50 phr	2.95	18.00	–	–	–
		1.00 phr	2.80	13.40	–	–	–
		5.00 phr	3.29	14.50	–	–	–
		10.00 phr	3.25	16.00	–	–	–
This work	BT	0 phr	2.72±0.12	60.5±1.7	3.85±0.56	–	3.82±0.08
		2 phr	3.15±0.10	62.3±1.3	4.56±0.29	18.44±5.90	4.33±0.09
		5 phr	3.45±0.15	64.2±2.6	8.02±0.68	108.31±15.66	4.65±0.07
		8 phr	3.62±0.09	65.8±2.1	11.24±0.71	191.95±23.19	5.20±0.10
		11 phr	3.98±0.05	68.0±1.6	10.21±0.42	165.19±16.72	5.17±0.08

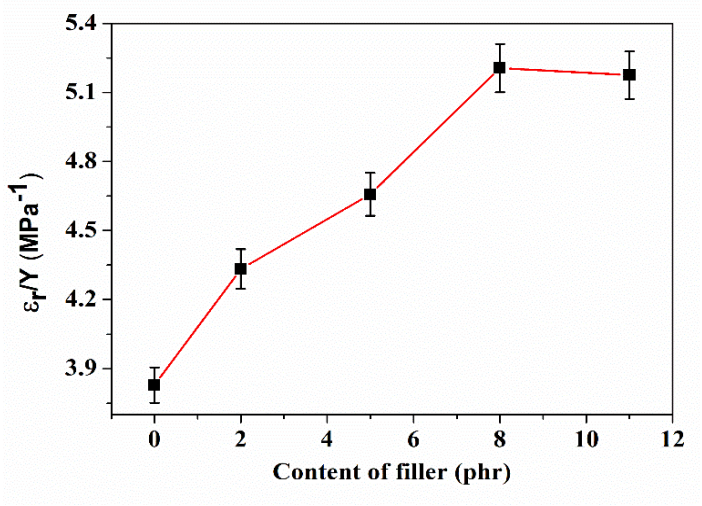

Figure 13: The ratio of dielectric constant to elastic modulus versus filler content of NR/BT composites filled with different contents of BT.

4. Conclusion

We aimed to fabricate natural rubber filled composites with enhanced dielectric constant and improved electromechanical properties which make them good candidates for applications in actuators and generators. It is successfully established that the addition of filler strongly improves mechanical, electrical, and electromechanical properties of NR/BT composites. From our experimental characterization and observations, 8 phr BT in NR is the optimum parameter resulting in the highest actuation strain of 11% with a dielectric constant of 4.1 at 1 Hz with minimum dielectric losses. Besides, dielectric breakdown is also enhanced from 60.5 MV/m to 68.0 MV/m. In this way, improved NR/BT composites furnish cost-effectiveness, high efficiency, improved properties that can be used for large scale industrial applications in the field of sensors, soft robotics, and energy harvesting.

References

[1] R. I. Haque, P. A. Farine, D. Briand, Sensors and Actuators A: Physical. **2018**, 271, 88-95

[2] R. Pelrine, R. Kornbluh, Q. Pei, J. Joseph, *Science* **2000**, 287, 836–9

[3] R. Pelrine, P. Sommer-Larsen, R. D. Kornbluh, R. Heydt, G. Kofod, Q. Pei, P. Gravesen, Smart Struct. Mater. 2001 Electroact. Polym. Actuators Devices **2001**, 4329, 335-49

[4] A. Gaur, P Maiti, In Reactive and Functional Polymers Volume Two, Springer, Cham, 2020, 325-347

[5] S. J. A. Koh, C. Keplinger, R. Kaltseis, C. C. Foo, R. Baumgartner, S. Bauer, Z. Suo, J. Mech. Phys. Solids **2017**, 105, 81–94

[6] D. Ahmad, K. Patra, M. Hossain, Contin. Mech. Thermodyn **2019**, 32, 489–500

[7] A. Kumar, D. Ahmad, K. Patra, J. Phys. Conf. Ser. **2019**, 1240, 18–22

[8] J. Guo, R. Xiao, H. S. Park, T. D. Nguyen, J. Appl. Mech. **2015**, 82(9), 091009

[9] R. Xiao, EPL (Europhysics Letters) **2016**, 114(1), 16002

[10] A. T. Mathew, S. J. A. Koh, Int. J. Smart Nano Mater. **2017**, 8**,** 214-231

[11] S. J. A. Koh, T. Li, J. Zhou, X. Zhao, W. Hong, J. Zhu, Z. Suo, J. Polym. Sci. Part B Polym. Phys. **2011**, 49**,** 504-515

[12] J. Sheng, H. Chen, J. Qiang, B. Li, Y. Wang, *J. Macromol. Sci. Part B* **2012**, 51, 2093–104

[13] A. O'Halloran, F. O'Malley, P. McHugh, J. Appl. Phys. **2008**, 104, 071101-9

[14] R. Pelrine, R. Kornbluh, G. Kofod, Adv. Mater. **2000**, 12, 1223–5

[15] Z. Liao, M. Hossain, X. Yao, M. Mehnert, P. Steinmann, *Int. J. Non. Linear. Mech.* **2020**, 118, 103263-78

[16] M. Mehnert, M. Hossain, P. Steinmann, Eur. J. Mech. A/Solids **2019**, 77, 103797-806

[17] P. Lotz, M. Matysek, H. F. Schlaak, IEEE/ASME Trans. Mechatronics **2011**, 16, 58–66

[18] G. Kofod, P. Sommer-Larsen, Sensors Actuators, A Phys. **2005**, 122, 273–83

[19] R. Kaltseis, C. Keplinger, S. J. A. Koh, R. Baumgartner, Y. F. Goh, W. H. Ng, A. Kogler, A. Tröls, C. C. Foo, Z. Suo, S. Bauer, RSC Adv. **2014**, 4, 27905–13

[20] D. Ahmad, S. K. Sahu, K. Patra, Polym. Test., **2019**, 79, 106038-49

[21] L. Jiang, Y. Zhou, S. Chen, J. Ma, A. Betts, S. Jerrams, J. Appl. Polym. Sci. **2018***,* 135, 6–11

[22] S. J. A. Koh, T. Li, J. Zhou, X. Zhao, W. Hong, J. Zhu, Z. Suo, *J. Polym. Sci. Part B Polym. Phys.* **2011**, 49, 504–15

[23] L. J. Romasanta, M. A. Lopez-Manchado, R. Verdejo, Prog. Polym. Sci, **2015***,* 51, 188–211

[24] P. Q. Zhang, J. H. Liu, H. D. Liu, F. Jia, Y. L. Zhou, J. Zheng, Appl. Phys. Lett. **2017**, 111, 1–4

[25] J. Qiang, H. Chen, B. Li, Smart Mater. Struct. **2012**, 21*,* 025006

[26] D. M. Opris, M. Molberg, C. Walder, Y. S. Ko, B. Fischer, Adv. Funct. Mater. **2011**, 21, 3531–9

[27] D. McCoul, S. Rosset, S. Schlatter, H. Shea, Smart Mater. Struct. **2017**, 26**,**

125022-39

[28] F. B. Madsen, A. E. Daugaard, S. Hvilsted, A. L. Skov, Macromol. Rapid Commun., **2016**, 37, 378–413

[29] A. Kumar, K. Patra, M. Hossain, Polym. Compos. **2020**, 42, 914-930

[30] W. P. Shih, L. L. Lee, C. W. Lee, L. C. Tsao, Y. J. Yang, K. C. Fan, J Chin Soc. Mech. Eng. **2011**, 32, 267-272.

[31] Z. Liao, M. Hossain, X. Yao, R. Navaratne, G. Chagnon, Poly. Test. **2020**, 86, 106478

[32] X. Guo, D. Xiang, G. Duan, P. Mou P, Waste Manag. **2010**, 30, 4–10

[33] K. Y. Volokh, Mechanics Research Communications **2010**, 37, 684-689.

[34] R. Malkapuram, V. Kumar, Y. S. Negi, Journal of reinforced plastics and composites **2009**, 28,1169-1189.

[35] Z. Suo, Acta Mech. Solida Sin. **2010**, 23, 549–78

[36] A. Tröls, A. Kogler, R. Baumgartner, R. Kaltseis, C. Keplinger, R. Schwödiauer, I. Graz, S. Bauer, Smart Mater. Struct. **2013**, 22, 104012

[37] R. Kaltseis, C. Keplinger, S. J. A. Koh, R. Baumgartner, Y. F. Goh, W. H. Ng, A. Kogler, A. Tröls, C. C. Foo, Z. Suo, S. Bauer, RSC Adv. **2014**, 4, 27905–13

[38] D. Yang, Y. Ni, X. Kong, H. Xue, W. Guo, L. Zhang, Appl. Surf. Sci. **2019**, 495, 143638

[39] G. Yin, Y. Yang, F. Song, C. Renard, Z. M. Dang, C. Y. Shi, D. Wang D, Appl. Mater. Interfaces **2017**, 9, 5237–43

[40] L. Jiang, A. Betts, D. Kennedy, S. Jerrams, Mater. Des. **2015**, **85** 733–42

[41] L. Duan, G. L. Wang, Y. Y. Zhang, Y. N. Zhang, Y. Y. Wei, Z. F. Wang, M. Zhang Polym. Compos. **2018**, 39, 691–7

[42] L. K. Namitha, M. T. Sebastian, Ceram. Int. **2017**, 43, 2994–3003

[43] C. Guo, M. Fuji, Adv. Powder Technol. **2016**, 27, 1162–72

[44] G. Yin, Y. Yang, F. Song, C. Renard, Z. M. Dang, C. Y. Shi, D. Wang, Appl. Mater. Interfaces **2017**, 9, 5237–43

[45] M. Ruan, D. Yang, W. Guo, S. Huang, Y. Wu, H. Wang, L. Zhang, RSC Adv. **2017**, 7, 37148–57

[46] D. Yang, Y. Xu, M. Ruan, Z. Xiao, W. Guo, H. Wang, L. Zhang, AIP Adv. **2019**, 9, 025035

[47] N. González, M. Custal, A. dels, G. N. Tomara, G. C. Psarras, J. R. Riba, E. Armelin, Eur. Polym. J. **2017**, 97, 57–67

[48] T. Jose, G. Moni, S. Salini, A. J. Raju, J. J. George, S. C. George, Ind. Crops Prod. **2017**, 105, 63–73

[49] S. Salaeh, A. Thitithammawong, Polym. Test. 2020, **85** 106417

[50] Y. J. Lee, P. Caspari, D. M. Opris, F. A. Nüesch, S. Ham, J. H. Kim, S. R. Kim, B. K. Ju, W. K. Choi, J. Mater. Chem. C, **2019**, 7, 3535–42

[51] A. Bele, M. Cazacu, G. Stiubianu, S. Vlad, RSC Adv. **2014**, 4, 58522–9

[52] M. Tian, J. Zhang, L. Zhang, S. Liu, X. Zan, T. Nishi, N. Ning, J. Colloid Interface Sci. **2014**, 430, 249–56

[53] S. Z. Salleh, H. Ismail, Z. Ahmad, J. Elastomers Plast. **2016**, 48, 640–55

[54] Y. Liu, L. Liu, Z. Zhang, J. Leng, Smart Mater. Struct. **2009**, 18**,** 095024-34

[55] M. Hossain, D. K. Vu, P. Steinmann, Arch. Appl. Mech. **2015**, 85, 523–37

[56] A. O'Halloran, F. O'Malley, P. McHugh, J. Appl. Phys. **2008**, 104**,** 071101-10

[57] P. J. Flory, J. Rehner, J. Chem. Phys. **1943**, 11, 512–20

[58] L. Bokobza, J. P. Chauvin, Polymer, **2005**, 46, 4144–51

[59] M. I. Aranguren, E. Mora, J. V. DeGroot, C. W. Macosko, J. Rheol. (N. Y. N. Y). **1992**, 36, 1165–82

[60] J. S. Plante, S. Dubowsky, Sensors Actuators, A Phys. **2007**, 137, 96–109

[61] R. Pelrine, R. Kornbluh, G. Kofod, Adv. Mater. **2000**, 12, 1223–1225

[62] I. Krakovský, T. Romijn, A. Posthuma de Boer, Journal of applied physics 85.1 (1999): 628-629.